Accepted Manuscript

Gelatin based films capable of modifying its color against environmental pH changes

Yanina S. Musso, Pablo R. Salgado, Adriana N. Mauri

Please cite this article as: Musso, Y.S., Salgado, P.R., Mauri, A.N., Gelatin based films capable of modifying its color against environmental pH changes, *Food Hydrocolloids* (2016), doi: 10.1016/j.foodhyd.2016.06.013.

Gelatin films added with acid-base indicators modify their color when being in contact with media of different pH:
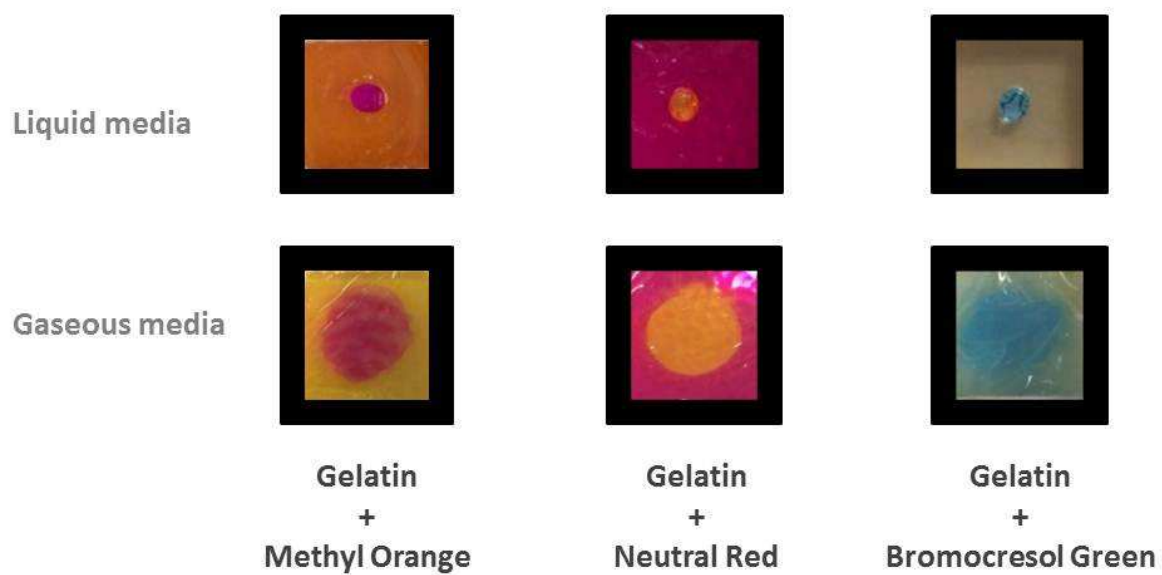
Liquid media

Gaseous media

Gelatin
+
Methyl Orange

Gelatin
+
Neutral Red

Gelatin
+
Bromocresol Green

1   **Gelatin based films capable of modifying its color against environmental pH**

2   **changes**

3

4   Yanina S. Musso, Pablo R. Salgado and Adriana N. Mauri[*]

5

6   Centro de Investigación y Desarrollo en Criotecnología de Alimentos (CIDCA),

7   CONICET CCT La Plata y Facultad de Ciencias Exactas, Universidad Nacional de La

8   Plata, 47 y 116 S/N°, (B1900JJ) La Plata, República Argentina.

9   Consejo Nacional de Investigaciones Científicas y Técnicas (CONICET), Av.

10   Rivadavia 1917, (C1033AAJ) Ciudad de Buenos Aires, República Argentina.

11

12   *Author to whom correspondence should be addressed: Tel.: +54-221-4249287; fax:

13   +54-221-4254853. E-mail: anmauri@quimica.unlp.edu.ar

14

15

16 **Abstract**

17 The aim of this work was to develop biodegradable protein-based films capable of sense

18 pH changes. These protein films were prepared by casting from aqueous solutions of

19 bovine gelatin, glycerol and three acid-base indicators: methyl orange (MO), neutral red

20 (NR) and bromocresol green (BCG), at pH 2, 6 and 11. All resulting protein films were

21 homogeneous, thin and had different colors depending on pH and the indicator used.

22 The response of these materials was evaluated simulating their contact with liquid and

23 semisolid media, and with a container headspace at acid and alkaline pH. In all tests,

24 developed protein films could modify their color after being in contact with media of

25 different pH. The physicochemical properties of films were also affected differently by

26 the presence of each acid-base indicator. While the addition of BCG did not

27 significantly modify the properties of control gelatin films, except its color; the

28 incorporation of MO and NR into film-forming solutions significantly improved

29 mechanical properties and decreased the water solubility and moisture content of the

30 resulting protein films without affecting their water vapor permeability.

31

33 **1. Introduction**

34 Innovations in food packaging technologies include the development of new active and

35 smart materials as well as the use of biopolymers as raw materials. These packaging

36 technologies attempts to ensure and extend the safety and quality of products during

37 shelf-life without affecting the environment, in response to new consumers` demands

38 (Brody, Bugusu, Han, Sand, & McHugh, 2008; Dainelli, Gontard, Spyropoulos,

39 Zondervan-van den Beuken, & Tobback, 2008; Restuccia et al., 2010).

40 Biopolymers-based systems can act as carriers of different types of additives. Thus,

41 numerous active packaging systems containing natural or synthetic antioxidant or

42 antimicrobials compounds, ethylene or oxygen captors, probiotics, flavors, etc., has

43 been developed (Campos, Gerschenson, & Flores, 2011; Mellinas et al., 2015; Salgado,

44 Ortiz, Musso, Di Giorgio, & Mauri, 2015; Silva-Weiss, Ihl, Sobral, Gómez-Guillén, &

45 Bifani, 2013). However, there are fewer studies on the development of smart systems

46 capable of monitoring the quality of the packaged food. They often attempt to sense

47 environmental changes or specific compounds generated during food packaging or

48 storage, in order to inform the freshness or microbiological quality of food to

49 manufacturers, retailers or consumers (Biji, Ravishankar, Mohan, & Srinivasa Gopal,

50 2015). Usually these smart devices provide qualitative information through visual

51 colorimetric changes and may be incorporated into the packaging materials or attached

52 to the inside or outside of the package (Ahvenainen, 2003; Biji, Ravishankar, Mohan, &

53 Srinivasa Gopal, 2015; Han & Scanlon, 2005; Kerry, 2008).

54

3

55 In this regard, the addition of synthetic acid-base indicators (bromocresol green, neutral

56 red, phenol red, bromocresol purple, cresol red, phenolphtalein, bromothymol blue,

57 xylenol blue, p-naphthol-benzein, hexamethoxy red, and their combinations) into

58 polymeric matrices such as polyvinyl alcohol, cellulose acetate, polyethylene and

59 polyethylene terephthalate has been studied by several authors to determine volatile

60 amines, CO_2, SO_2 and other byproducts of bacterial growth (Booher & Gorski, 2011;

61 Eagland, 2004; Gorski & Booher, 2011; Pacquit et al., 2006, 2007). The above-

62 mentioned indicators have been used as model systems since they are not GRAS

63 compounds, but recently some natural compounds, such as grape, flowers and spinach

64 extracts or anthocyanins have been proved to be capable to react to external pH stimuli

65 (Maciel, Yoshida, & Franco, 2015; Veiga-Santos, Ditchfield, & Tadini, 2011; Zhang,

66 Lu, & Chen, 2014).

67 Even though many plant and animal proteins have been used as raw material for

68 producing active packaging (Campos, Gerschenson, & Flores, 2011; Mellinas et al.,

69 2015; Salgado, Ortiz, Musso, Di Giorgio, & Mauri, 2015; Silva-Weiss, Ihl, Sobral,

70 Gómez-Guillén, & Bifani, 2013; Mauri & Añon, 2012; Mauri, Salgado, Condés, &

71 Añón in press), as far as we know, there is no literature related to the formation of pH

72 colorimetric indicator films based on proteins.

73 Proteins are heteropolymers of α-amino acids which differ in their side groups. As they

74 can act as buffer systems due to their ionizable side groups, their film´s responsiveness

75 to pH changes is uncertain. Moreover, the aminoacids' side groups could be highly

76 reactive against potential cross-linking or chemical grafting (Guilbert & Gontard, 2005).

77 This potential reactivity could inactivate additives added to the formulation to provide a

78 new functionality, or change protein network cross-linking, thus affecting the

79 physicochemical properties of films.

4

80   In this context, the aim of the present work was to develop protein films capable of

81   sensing pH changes through the addition of acid-base indicators to film formulations.

82   Gelatin was selected as protein source since their films are colorless (Gómez-Guillén et

83   al., 2009) – unlike plant protein based films which generally present certain color,

84   inherent to non-protein compounds extracted together with proteins (Salgado, Molina

85   Ortiz, Petruccelli, & Mauri, 2010). This colorless would allow films to take the

86   indicator color without interference. Three synthetic acid-base indicators, with different

87   chemical structure and significant color variations in a wide pH range, were selected as

88   system models to activate protein films.

89

90   **2. Material and Methods**

91

92   **2.1 Materials**

93   Bovine gelatin with 240 Bloom (Kraft Foods, Argentina) was used as protein source. Its

94   protein content, as measured by the Kjeldahl method (AOAC, 1995), was $87.8 \pm 0.6\%$

95   (w/w, dry weight; $N \times 5.5$). Glycerol (Anedra, Argentina) was used as film plasticizer.

96   Three acid-base indicators were employed: methyl orange (MO, Benzenesulfonic acid,

97   4-[[(4-dimethylamino)phenyl]azo]-, sodium salt, Mallinckrodt Baker, USA), neutral red

98   (NR, 2,8-Phenazinediamine,N8,N8,3-trimethyl-, monohydrochloride, Pablo Zubizarreta

99   Ward, Argentina) and bromocresol green (BCG, Phenol, 4,4´-(2,2-dioxido-3H-1,2-

100   benzoxathiol-3-ylidene)*bis*[2,6-dibromo-3-methyl],   monosodium   salt,   Anedra,

101   Argentina). **Table 1** shows their chemical structures, pKa values, pH dependence color,

102   and λ_{max} in the visible region (Sabnis, 2007). All the other reagents used in this study

103   were of analytical grade.

104

5

2.2 Films preparation

Films were prepared by casting. Initially two aqueous solutions were prepared by magnetic stirring, one containing 10% (w/v) gelatin at 100°C and the other containing 2.5 % (w/v) glycerol plus 0.04% (w/v) methyl orange, neutral red or bromocresol green (MO, NR and BCG respectively) at room temperature. Equal volumes of both solutions were then mixed by stirring for additional 30 min at room temperature and the pH was adjusted to 2, 6 and 11, with 2 mol/L HCl or 2 mol/L NaOH. Finally, 10 mL of each film-forming solution were cast onto polystyrene Petri dishes ($64\,cm^2$) and dried in an oven with air flow circulation (Yamato, DKN600, USA) at 60ºC for 3 h. Resulting films were preconditioned 48 h at 20ºC and 58% relative humidity (in desiccators with saturated solutions of NaBr) just before being peeled from the casting surface and characterized.

Furthermore, control gelatin films without the incorporation of acid-base indicators into film-forming solutions, at pH= 2, 6 and 11, were obtained as described previously.

Three independent batches for each type of protein film (G, G+MO, G+NR, and G+BCG) were performed.

2.3 Films characterization

Thickness: Film thickness was measured by a digital coating thickness gauge (Check Line DCN-900, USA). Measurements were done at five positions along the rectangular strips for the tensile test, and at the center and at eight positions round the perimeter for the water vapor permeability (WVP) determinations. The mechanical properties and WVP were calculated using the average thickness for each film replicate.

128 *Moisture content (MC):* Small specimens of films were collected after conditioning, cut

129 and weighed before and after oven drying at 105°C for 24 h, ASTM D644-99, (ASTM

130 2004). MC values were determined in triplicate for each film, and calculated as the

131 percentage of weight loss relative to the original weight.

132 *Color:* Film color was determined with a Konica Minolta Chroma Meter CR-400

133 (Konica Minolta Chroma Co., Osaka, Japan) set to C illuminant/2° observer. A CIE-Lab

134 color scale was used to measure the degree of lightness (*L**), redness (+*a**) or greenness

135 (-*a**), and yellowness (+*b**) or blueness (-*b**) of the films. The instrument was

136 calibrated using a white standard plate with color coordinates of $L^*_{standard}$ = 97.55,

137 $a^*_{standard}$ = -0.03 and $b^*_{standard}$ = 1.73 provided by Minolta. Films color was measured on

138 the surface of this standard plate and total color difference (*ΔE**) was calculated as

139 follow:

140 $\Delta E^* = [(L^*_{film} - L^*_{standard})^2 + (a^*_{film} - a^*_{standard})^2 + (b^*_{film} - b^*_{standard})^2]^{0.5}$ (1)

141 Values were expressed as the means of nine measurements on different areas of each

142 film.

143 *Visible absorption spectra:* Each film specimen was cut into a rectangular piece and

144 placed directly in a spectrophotometer test cell. A spectrum (from 400 to 800 nm) of

145 each film was obtained in an UV-Vis spectrophotometer (Beckman DU650, Germany).

146 Measurements were performed using air as reference. All determinations were

147 performed in triplicate.

148 *Water vapor permeability (WVP):* Water vapor permeability tests were conducted

149 according to ASTM method E96-00 (ASTM, 2004) with some modifications. Each film

150 sample was sealed over a circular opening of 0.00185 m^2 in a permeation cell that was

151 stored at 20°C in desiccators. To maintain a 75% relative humidity (RH) gradient across

7

152   the film, anhydrous silica (0% RH_c) was placed inside the cell and a saturated NaCl

153   solution (75% RH_d) was used in the desiccators. The RH inside the cell was always

154   lower than outside, and water vapor transport was determined from the weight gain of

155   the permeation cell. When steady-state conditions were reached (about 1 h), eight

156   weight measurements were made over 5 h. Changes in the weight of the cell were

157   recorded and plotted as a function of time. The slope of each curve ($\Delta m/\Delta t$, g H_2O s^{-1})

158   was obtained by linear regression and the water vapor transmission rate (WVTR) was

159   calculated from the slope divided by the permeation cell area (A, in m^2). WVP (g H_2O

160   Pa^{-1} s^{-1} m^{-1}) was calculated as:

161                   $$WVP = [WVTR / (P_V^{H2O} \cdot (RH_d - RH_c))] \cdot d \qquad (2)$$

162   Where: WVTR = water vapor transmission rate (g H_2O s^{-1} m^{-2}), P_V^{H2O} = saturation

163   water vapor pressure at test temperature (2339.27 Pa at 20 °C), RH_d - RH_c = relative

164   humidity gradient across the film -expressed as a fraction- (0.75), A = permeation area

165   (m^2), and d = film thickness (m). Each WVP value represents the mean value of three

166   samples taken from different films.

167   *Water solubility (WS):* WS was determined as was described by Gontard, Duchez, Cuq,

168   & Guilbert (1994) with slight modifications. Three pieces of films were weighed

169   (diameter = 2 cm; ~0.03-0.05 g) and immersed in 50 mL of distilled water. The system

170   was sealed, shaken at 100 rpm for 24 h at 20°C (Ferca, TT400 model, Argentina), and

171   then filtered through Whatman n°1 filter paper (previously dried and weighed) to

172   recover the remaining undissolved film, which was desiccated at 105°C for 24 h. WS

173   was calculated as follows:

174              $$WS = [(P_0 \cdot (100 - MC)) - P_f] \cdot 100 / [P_0 \cdot (100 - MC)] \qquad (3)$$

175   Where P_0 = initial film weight (g), P_f = final dry film weight (g), MC = moisture content

176   (%). All tests were carried out in triplicate.

177   *Glass transition temperature (Tg):* Tg was determined by differential scanning

178   calorimetry, using a DSC TA 2010 calorimeter Q100 V9.8 Build 296 (TA Instrument,

179   New Castle, Del., USA) controlled by a TA 5000 module with a quench cooling

180   accessory. Temperature and heat flow calibration of the equipment were carried out

181   according to ASTM methods, using lauric and stearic acids and indium as standards.

182   Hermetically sealed aluminum pans containing 5 mg of films were prepared, and the

183   capsules were scanned at 10°C/min over the range -80 to 150°C. Tg, defined as the

184   inflexion point of the base line, caused by the discontinuity of the specific heat of the

185   sample (ASTM D3418-03 (ASTM, 2004)), was calculated using the Universal Analysis

186   V4.2E software (TA Instruments, New Castle, Del., USA). All the assays were

187   performed at least in duplicate.

188   *Mechanical properties:* Tensile strength (TS), elastic modulus (EM) and elongation at

189   break (EAB) of films were determined following the procedures outlined in the ASTM

190   method D882-02 (ASTM, 2004), using a texture analyzer TA.XT2i (Stable Micro

191   Systems, Surrey, England) equipped with a tension grip system A/TG. Films probes of

192   90 mm length and 6 mm width were used. The initial grip separation was set at 50 mm

193   and the crosshead speed at 0.4 mm s^{-1}. Measurements were made at 20°C in a

194   temperature-controlled room.

195   The curves of force (N) as a function of distance (mm) were recorded by the Texture

196   Expert V.1.15 software (Stable Micro Systems, Surrey, England). Tensile properties

197   were calculated from the plot of stress (tensile force/initial cross-sectional area) versus

198   strain (extension as a percentile of the original length). TS and EAB were determined

199   directly from the stresses-train curves, and EM was determined as the slope of the initial

200   linear portion of this curve. Reported values are the average of at least twelve

201   replications taken from different films for each formulation.

202 **2.4 Films' response to pH changes**

203 Each film was faced with liquid, semisolid and gaseous media of different pH: i) adding

204 a drop of 2 mol/L HCl or 2 mol/L NaOH directly on films; ii) placing the films in

205 contact with gels prepared from gelatin solutions at 7.5% w/v at pH= 2.5, and 11; and

206 iii) exposing the films to gaseous atmospheres generated by acetic acid glacial ($C_2H_4O_2$,

207 pK_a~4.8, Anedra, Argentina) and ammonia (NH_3, pK_a~9.3, Anedra, Argentina).

208 Photographs of films before and after (30 minutes) contacting it with those media of

209 different pH were taken with a digital camera (Kodak M853, USA) and color variations

210 were measured using a colorimeter (Konica Minolta Chroma Meter CR-400), as

211 described above, at the same time films were photographed.

212

213 **2.5 Statistical analysis**

214 Results were analyzed by two-way ANOVA (two factors: pH and presence of acid-base

215 indicator, in three and four levels, respectively: pH=2, 6 and 11; control films (G) and

216 those added with MO, NR and BCG (G+MO, G+NR and G+BCG, respectively). Means

217 were tested with the Tukey's HSD (honestly significant difference) test for paired

218 comparison, with a significance level α=0.05, using the Statgraphics Plus version 5.1

219 software (Statgraphics, USA).

220

221 **3. Results and Discussion**

222 *3.1 Appearance and optical properties of films*

223 All gelatin films prepared with or without methyl orange, neutral red and bromocresol

224 green acid-base indicators at pH 2, 6 and 11 were homogeneous, thin, flexible, and

225 transparent. **Figure 1** shows their visual appearance. Control gelatin films (**G**) were

226 clear and colorless for all pHs tested. The addition of methyl orange (MO), neutral red

10

227 (NR) and bromocresol green (BCG) to film-forming solutions allowed to obtain

228 transparent films with different and well defined colors, dependent on the nature of each

229 acid-base indicator and the solutions pH (2, 6, and 11). Even the color of films matches

230 to the inherent color of the indicators at each pH, reported in **Table 1**. Color parameters

231 (*L**, *a**, *b** and *ΔE**) and the absorption spectra in the visible range of protein films are

232 shown in **Table 2** and **Figure 2** respectively. Regardless of the pH of the film-forming

233 solutions, control gelatin films (**G**) showed a high brightness (high *L**), absence of color

234 (low values of *a**, *b**, and ΔE*) (p>0.05), and no signal in their absorption spectra in

235 the visible range (data not shown). But these protein films acquired a specific coloration

236 with the addition of the acid-base indicators to the formulations, characterized by

237 different values of *a** and *b**, and a significant lower brightness than **G** films (p<0.05).

238 The absorption spectra of these colored films showed peaks at different wavelengths in

239 the visible range, which were related to their colorations. Gelatin films incorporated

240 with MO (**G+MO**) were orange at pH 2, yellow at pH 6, and purple at pH 11, with

241 maximum absorptions (λ_{max}) at 510 nm, 430 nm, and 570 nm in their respective spectra

242 (**Figure 2.A**). It is worth noting that films with MO at alkaline pH showed a purple

243 color not reported for this indicator in the cited literature (Sabnis, 2007). On the other

244 hand, gelatin films incorporated with NR (**G+NR**) were yellow at pH 11, and purple at

245 pH≤6, with λ_{max} at 460 nm and 520 nm in their respective visible spectra (**Figure 2B**).

246 But it is possible to note, that those films prepared at pH 2 showed a higher absorption

247 peak and a higher intensity of the hue (with higher values of *a** and lower values of *b**)

248 than those prepared at pH 6. Finally, gelatin films incorporated with BCG (**G+BCG**)

249 were barely yellow at pH 2 and blue at pH 6 and 11, with maximum absorptions at 440

250 nm and 620 nm respectively (**Figure 2C**). For this indicator, films at pH 11 showed a

11

251 more intense coloration than those at pH 6, evidenced by an increase in its absorption

252 peak, a more negative $b*$ value and a higher $a*$ value.

253 Coloration of films could be considered as an additional attribute for some commercial

254 applications. These materials can act as barriers to visible light, protecting food

255 products from oxidation (Cian, Salgado, Drago, González, & Mauri, 2014).

256

257 *3.2 Films´ response to pH changes*

258 **Figure 3** shows the response of all developed films when placed in contact with acid

259 and alkali liquids, semisolids and gases. This assay allows verifying the ability of these

260 films to sense pH changes, simulating that these changes could occur in a liquid or

261 semisolid food, or in the headspace of a food container as the result of the reaction

262 products of food spoilage. Thus, the material could inform indirectly about the quality

263 and safety of the product during its storage and distribution chain until be consumed.

264 All color changes seen in **Figure 3**, which were reversible, were confirmed by

265 colorimetric measurements. Hunter color parameters L*, a* and b* are shown as

266 supplementary material.

267 Gelatin films incorporated with MO, NR, and BCG could change their color after being

268 in contact with alkali or acid solutions of NaOH or HCl respectively, gaseous

269 atmospheres of acetic acid or ammonia, and gelatin gels at pH 2.5 and 11, except for

270 those in which the pH of the medium and film were similar. These film responses were

271 immediately and markedly with liquid and gases of different pH, but less evident and

272 slower with semisolid media. Slower turning kinetics of acid-base indicators against

273 semisolid media could probably be attributed to limited diffusive processes.

274 **Figure 3.A** shows changes in color of gelatin films incorporated with MO (**G+MO**)

275 after being in contact with different pH media. For example, films obtained at pH 6

276   resulted initially yellow, but became orange or purple by placing a drop of HCl or

277   NaOH solutions on them respectively. The same behavior was observed when the films

278   were exposed to acidic or alkaline gaseous atmospheres. It is noteworthy that acidic

279   gaseous atmosphere produced by acetic acid did not alter the color of the yellow film at

280   pH 6 and turned purple to yellow film at pH 11, not reaching the characteristic orange

281   color of MO in acidic medium. This could be attributed to the pKa of acetic acid (pKa ~

282   4.8) that is higher than the pH at which MO turns to its acid form (pKa=3.7).

283   Films at pH 6 and 11 in contact with semisolid medium at pH 2.5 veered to the same

284   yellow acquired by acidic films, instead of the expected orange coloration. This could

285   be attributed to the diffusion of the indicator to the gel during the assay, which also

286   provided color to the media. Meanwhile against semisolid media at pH 11, films at pH 6

287   reached the alkaline purple coloration, but those of pH 2 turned yellow. It seemed that

288   these acid films failed to achieve the pH of the gel or that their structural characteristics

289   favored the diffusion of the indicator, according to the observations previously

290   mentioned.

291   **Figure 3.B** shows how gelatin films with NR in their formulation (**G+NR**) could sense

292   the pH of the surrounding medium. They modified their color by placing a drop of acid

293   or alkali on them or when subjected to acidic or alkaline gaseous atmospheres. As noted

294   above, the changes in films color were less evident when they were contacted with

295   semisolids, at different pHs.

296   Gelatin films incorporated with BCG (**G+BCG**) showed similar behavior than **G+NR**

297   films (**Figure 3.C**). They changed their color clearly and immediately after being in

298   contact with acid and alkaline liquids and gaseous media. These color changes were

299   very noticeable since the films turned from barely yellow (at acidic pH) to blue (at

300   neutral or alkaline pH) or vice versa, being these changes less evident when films were

301   contacted with semisolid media.

302   Microbial growth often influence the pH of the medium due to metabolites produced by

303   microorganisms, for example lactic acid, hydrogen sulfide, volatile amines, etc. (Biji,

304   Ravishankar, Mohan, & Srinivasa Gopal, 2015; Han & Scanlon, 2005; Kerry & Butler,

305   2008). If packaging material could sense this change through a change in its color, it

306   would inform producers, sellers and consumers about the quality and safety of the

307   packaged food (Biji, Ravishankar, Mohan, & Srinivasa Gopal, 2015; Kerry & Butler,

308   2008)

309

310   *3.3 Effect of pH and acid-base indicators addition on the physicochemical properties of*

311   *films*

312   Regardless of the presence of acid-base indicators in formulations, pH of film-forming

313   solutions affects the ionization state and the conformation of proteins, thus conditioning

314   the interactions that can occur between polypeptide chains and among proteins and

315   other components during film formation. Protein–protein interactions involved in film

316   matrix stabilization determine the cross-linking degree and the hydrophylic-

317   hydrophobic character of the films, which correlate with their physicochemical,

318   mechanical, and barrier properties (Mauri & Añón, 2006, 2008). Furthermore, the

319   incorporation of additives into materials formulation attempting to confer specific

320   functionalities on films –such as antioxidants, antimicrobials, vitamins,

321   microorganisms, probiotics, flavors, and pigments– could also affect protein cross-

322   linking and therefore modify the physicochemical properties of the resulting materials

323   (Salgado, Ortiz, Musso, Di Giorgio, & Mauri, 2015; Mauri , Salgado, Condés & Añón

324   in press).

14

325 Thickness, moisture content (MC), water solubility (WS), water vapor permeability

326 (WVP) and glass transition temperature (Tg) of developed films are showed in **Table 3.**

327 No modification in films thickness (~ 50 μm) was observed with the addition of acid-

328 base indicators used (p>0.05) neither with the pH of the film-forming dispersion

329 (p>0.05). Moisture content of control gelatin films (**G**) –without acid-base indicator

330 addition– were ~20%. The addition of **MO** and **NR** into formulations significantly

331 decreased the moisture content of the resulting films (**G+MO** and **G+NR**) (p<0.05) at

332 all studied pH, while the incorporation of **BCG** did not modify their moisture content

333 respect to **G** films (p>0.05). Variation on pH only modified the moisture content of **G**

334 and **G+BCG** films (p<0.05) slightly. In both cases, films obtained at pH 6 shows the

335 highest MC values (p<0.05).

336 Control gelatin films (**G**) showed interesting water solubilities –between 37 and 49 %

337 depending on the pH of film-forming solutions – which resulted lower than others

338 values reported in the literature for this protein films (Nur Hanani, Roos, & Kerry,

339 2012). The addition of the acid-base indicators into the formulations caused different

340 effects on the water solubility of the resulting films. **MO** provoked a significantly

341 decrease in water solubility of the resulting films (p<0.05), being this effect higher at

342 pH 11 (*ca.* 60%) than at pH 2 and 6 (*ca.* 40%). **NR** did not affect the water solubility of

343 gelatin films (p>0.05) and **BCG** caused differential behaviors on water solubility

344 depending on the pH of the film-forming solutions: increased it ~25% at pH=11

345 (p>0.05), decreased it ~40% at pH=6 (p>0.05), and did not modify it at pH=2 (p<0.05).

346 Control gelatin films and those colored by **MO** and **NR** prepared at acidic pH were

347 more soluble than those obtained at neutral or alkaline pH (p<0.05). But those colored

348 by **BCG** showed similar water solubilities at pH 2 and 11, higher than at pH 6 (p<0.05).

15

349 These results suggest a different protein cross-linking degree dependent on the presence

350 of the acid-base indicators and pH of film-forming solutions.

351 Unlike water solubility and moisture content results, no significant differences in water

352 vapor permeability (WVP) of films were observed (~8.2 10^{-11} g H_2O s^{-1} m^{-1} Pa^{-1}) with

353 the addition of acid-base indicators (p>0.05) or changing the pH of film-forming

354 solutions (p>0.05).

355 Mechanical properties of developed gelatin films are presented in **Figure 4**. Control

356 gelatin films (**G**) showed moderate tensile strength (TS), Young´s modulus (EM), and

357 elongation at break (EAB). These properties were affected by both the presence and

358 type of acid-base indicator (p<0.05) as by the initial pH of protein dispersion (p<0.05).

359 Incorporation of **MO** or **NR** into formulations improved the mechanical properties of

360 these materials. This colored films showed higher tensile strength and Young´s modulus

361 but lower elongation at break than control films (**G**) (p<0.05). These improvements

362 were most notable at neutral and alkaline pH than at acidic pH. **G+NR** films showed the

363 best mechanical properties of films developed. In particular, addition of **NR** to gelatin

364 film-forming solutions at pH=11 markedly increased tensile strength (*ca.* 400%) and

365 Young´s modulus (*ca.* 2000%) of resulting films (p<0.05), in detriment of its elongation

366 at break (*ca.* 40% decrease) (p<0.05). Moreover, **G+BCG** films had similar mechanical

367 properties than respective control films (p>0.05). And it is worth noting that gelatin-

368 based films added or not with different acid-base indicators obtained at pH 6 and 11

369 showed higher tensile strength than those prepared from acidic film-forming solutions

370 (p<0.05).

371 These results suggest that studied acid-base indicators, with different chemical

372 structures (shown in **Table 1**), could interact differently with gelatin in the protein

373 network. Addition of **MO** and **NR** to formulations seems to favor protein cross-linking,

16

374 leading to more resistant and less water soluble films, with lower moisture content and

375 without affecting their water vapor permeability. Whereas **BCG** addition seems not

376 interfere in protein matrixes obtained at pH 6 and 11, but favor certain plasticizing

377 effect in acidic films.

378 Glass transition temperatures (Tg) of studied films are presented in **Table 3**. All films

379 showed just one Tg, suggesting that no phase separation was

380 observed (Tapia-Blácido, Mauri, Menegalli, Sobral, and Añón, 2007). Neither the

381 presence and type of acid-base indicators nor pH of the film-forming solutions modified

382 Tg of the materials (p>0.05), except for **G+MO** and **G+BCG** films at pH 6 that showed

383 slightly higher Tg than control films (p<0.05). These results did not represent the

384 greater cross-linking or the possible plasticizing effect on protein matrix suggested

385 above when analyzing moisture content, water solubility and mechanical properties of

386 films. The different moisture content of films also is affecting the Tg value. These

387 results suggest that **MO** and **NR** molecules could be acting as physical and/or chemical

388 entanglements not modifying the mobility of polypeptide chains.

389

390 **4. Conclusions**

391 Gelatin-based films capable of sensing changes in the surrounding pH medium were

392 developed by addition of methyl orange, neutral red and bromocresol green –known

393 acid-base indicators– in their formulation. All films modified its color reversibly when

394 they were in contact with liquid, gaseous and semisolid media of different pHs. The

395 addition of these compounds also modifies the physicochemical properties of the

396 resulting materials. In particular, methyl orange and neutral red could be acting as

397 physical and/or chemical entanglements, increasing the tensile strength and reducing the

398 water solubility of the resulting films, without affecting their water vapor permeability

17

399 and their capacity to change their color against the pH of the surrounding medium.

400 These smart materials, used as food packaging or coatings, could inform about the

401 safety and quality of any product whose deterioration mode caused a change in the pH

402 of the media, such as microbial growth.

403 Evidence that the protein matrix did not interfere with the discoloration of the acid-base

404 indicators when being in contact with a medium of different pH, pushed to find food

405 grade dyes that could replace the synthetic ones analyzed in this work and to probe this

406 materials as packaging of real systems.

407

412

413 **References**

414 Ahvenainen, R. (2003). *Novel food packaging techniques*. Elsevier Ltd.

415 AOAC.(1995). *Official methods of analysis of AOAC international.* (16th ed.),

416 Horowitz, Washigton DC, USA.

417 ASTM. (2004). *Annual book of ASTM standards*. ASTM International: Philadelphia,

418 PA, USA.

419 Biji, K. B., Ravishankar, C. N., Mohan, C. O., & Srinivasa Gopal, T. K. (2015). Smart

420 packaging systems for food applications: a review. *Journal of Food Science and*

421 *Technology*, 52, 6125-6135.

422 Booher J, GorskiJ. R. (2011). Polymeric indicators for detecting the presence of

423 metabolic byproducts from microorganisms. Patent US20110042344.

424 Brody, A. L., Bugusu, B., Han, J. H., Sand, C. K., & McHugh, T. H. (2008). Innovative

425 food packaging solutions. *Journal of Food Science*, 73, R107-R116.

426 Campos, C., Gerschenson, L., & Flores, S. (2011). Development of edible films and

427 coatings with antimicrobial activity. *Food and Bioprocess Technology*, 4, 849–875.

428 Cian, R. E., Salgado, P. R., Drago, S. R., González, R. J., & Mauri, A. N. (2014).

429 Development of naturally activated edible films with antioxidant properties prepared

430 from red seaweed *Porphyra columbina* biopolymers. *Food Chemistry*, 146, 6–14.

431 Dainelli, D., Gontard, N., Spyropoulos, D., Zondervan-van den Beuken, E., & Tobback,

432 P. (2008). Active and intelligent food packaging: legal aspects and safety concerns.

433 *Trends in Food Science and Technology*, 19, S103–S112.

434 Eagland D. (2004). Polymeric materials incorporating a pH indicator dye. Patent

435 US20070276207.

436 Gómez-Guillén, M. C., Pérez-Mateos, M., Gómez-Estaca, J., López-Caballero, E.,

437 Giménez, B., & Montero, P. (2009). Fish gelatin: a renewable material for developing

438 active biodegradable films. *Trends in Food Science & Technology*, 20, 3–16.

439 Gontard, N., Duchez, C., Cuq, J., & Guilbert, S. (1994). Edible composite films of

440 wheat gluten and lipids - water-vapor permeability and other physical-properties.

441 *International Journal of Food Science and Technology*, 29, 39–50.

442 GorskiJ. R., BooherJ. (2011). Processes for preparing a polymeric indicator film. Patent

443 US20110274593.

444 Guilbert, S., & Gontard, N. (2005). Agro-polymers for edible and biodegradable films.

445 Review of agricultural polymeric materials, physical and mechanical characteristics.

446 *Innovations in Food Packaging*, 263–276.

447 Han, J., & Scanlon, M. (2005). Mass transfer of gas and solute through packaging

448 materials. In Han, J. (Ed.). *Innovations in food packaging* (pp. 12–23). Elsevier

449 Academic Press.

450 Kato, E. T., Yoshida, C. M., Reis, A. B., Melo, I. S., & Franco, T. T. (2011). Fast

451 detection of hydrogen sulfide using a biodegradable colorimetric indicator system.

452 *Polymer International*, 60, 951–956.

453 Kerry J. & Butler, P. (2008). *Smart packaging technologies for fast moving consumer*

454 *goods*. J. Wiley.

455 Maciel, V. B. V., Yoshida, C. M. P., & Franco, T. T. (2015). Chitosan/pectin

456 polyelectrolyte complex as a pH indicator. *Carbohydrate Polymers,*132, 537-545.

457 Mauri A. N. & Añon M. C. (2012). Proteínas como envases alimentarios. In Olivas

458 Orozco G.I., González-Aguilar G.A., Martín-Belloso O. and Soliva-Fortuny R.

459 Películas y recubrimientos comestibles: propiedades y aplicaciones en alimentos. (pp.

460 95-124). Editorial Clave.

461 Mauri A. N., Salgado P.R., Condés M.C & Añón M.C. (in press). Films and coatings

462 from vegetable proteins. In Montero M.P, Gómez-Guillén M.C., López-Caballero M.E.

463 &. Barbosa-Cánovas G.V. (Eds.). Edible films and coatings: Fundamentals and

464 applications. CRC Press, Taylor & Francis Group.

465 Mauri, A. N., & Añón, M. C. (2006). Effect of solution pH on solubility and some

466 structural properties of soybean protein isolate films. *Journal of Science of Food and*

467 *Agriculture*, 86, 1064–1072.

468 Mauri, A. N., & Añón, M. C. (2008). Mechanical and physical properties of soy protein

469 films with pH-modified microstructures. *Food Science and Technology International*,

470 14, 119–125.

471 Mellinas, C., Valdés, A., Ramos, M., Burgos, N., Garrigós, M. del C., & Jiménez, A.

472 (2015). Active edible films: Current state and future trends. *Journal of Applied Polymer*

473 *Science*, 132, 42631.

474 Nur Hanani, Z. A., Roos, Y. H., & Kerry, J. P. (2012). Use of beef, pork and fish gelatin

475 sources in the manufacture of films and assessment of their composition and mechanical

476 properties. *Food Hydrocolloids*, 29, 144–151.

477 Pacquit, A., Lau, K. T., McLaughlin, H., Frisby, J., Quilty, B., & Diamond, D. (2006).

478 Development of a volatile amine sensor for the monitoring of fish spoilage. *Talanta*, 69,

479 515–20.

480 Pacquit, A., Frisby, J., Diamond, D., Lau, K., Farrell, A., Quilty, B., & Diamond, D.

481 (2007). Development of a smart packaging for the monitoring of fish spoilage. *Food*

482 *Chemistry*, 102, 466–470.

483 Restuccia, D., Spizzirri, U. G., Parisi, O. I., Cirillo, G., Curcio, M., Iemma, F., & Picci,

484 N. (2010). New EU regulation aspects and global market of active and intelligent

485 packaging for food industry applications. *Food Control*, 21, 1425–1435.

486 Sabnis R.W. (2007). *Handbook of acid-base indicators*.CRC Press.

487 Salgado, P. R., Molina Ortiz, S. E., Petruccelli, S., & Mauri, A. N. (2010).

488 Biodegradable sunflower protein films naturally activated with antioxidant compounds.

489 *Food Hydrocolloids*, 24, 525–533.

490 Salgado, P. R., Ortiz, C. M., Musso, Y. S., Di Giorgio, L., & Mauri, A. N. (2015).

491 Edible films and coatings containing bioactives. *Current Opinion in Food Science*, 5,

492 86–92.

493 Silva-Weiss, A., Ihl, M., Sobral, P. J. A., Gómez-Guillén, M. C., & Bifani, V. (2013).

494 Natural additives in bioactive edible films and coatings: functionality and applications

495 in foods. *Food Engineering Reviews*, 5, 200–216.

496 Tapia-Blácido D., Mauri A.N., Menegalli F.C., Sobral P.J.A., & Añón M.C. (2007).

497 Contribution of the starch, protein, and lipid fractions to the physical, thermal, and

498 structural properties of amaranth (*Amaranthus caudatus*) flour films. *Journal of Food*

499 *Science*, 72, 293-300.

500 Veiga-Santos P., Ditchfield C., Tadini C.C. (2011). Development and evaluation of a

501 novel pH indicator biodegradable film based on cassava starch. *Journal of Applied*

502 *Polymer Science,* 120, 1069-1079.

503 Zhang, X., Lu, S., & Chen, X. (2014). A visual pH sensing film using natural dyes from

504 *Bauhinia Blakeana Dunn*. *Sensors and Actuators B: Chemical*, 198, 268–273.

505

506 **Figure legends**

507

508 **Figure 1.** Appearance of control gelatin-based films (G) and those added with methyl

509 orange (G+MO), neutral red (G+NR), and bromocresol green (G+BCG) at pH 2, 6 and

510 11.

511

512 **Figure 2.** Visible absorption spectra (400-800 nm) of gelatin-based films added with

513 methyl orange (**A**), neutral red (**B**) and bromocresol green (**C**) at pH 2, 6, and 11

514 respectively.

515

516 **Figure 3.** Response of gelatin-based films added with methyl orange (G+MO, **A**),

517 neutral red (G+NR, **B**), and bromocresol green (G+BCG, **C**) at pH 2, 6 and 11 after

518 being in contact with liquid, gaseous and semisolid media of different pHs.

519

520 **Figure 4.** Mechanical properties of gelatin-based films obtained at different pH (2, 6

521 and 11) added or not with different acid-base indicators (MO, NR, and BCG). **A**)

522 Tensile strength (TS). **B**) Young´s modulus (EM). **C**) Elongation at break (EAB).

523

524 **Table captions**

525

526 **Table 1.** Chemical structure, pKa, pH dependence color, and λ_{max} in the visible region

527 of methyl orange (MO), neutral red (NR) and bromocresol green (BCG), used in this

528 manuscript as pH indicators.

23

529

530 **Table 2.** CIE-Lab color parameters (*L*, a** and *b**) and total color difference (*ΔE**) of

531 gelatin-based films added or not with different acid-base indicators (MO, NR, BCG)
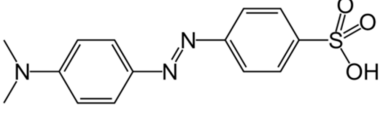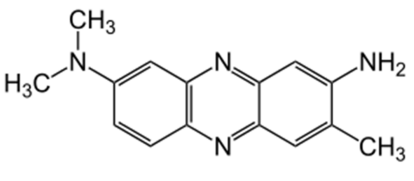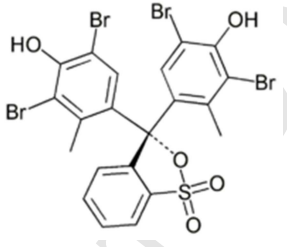
532 obtained at different pH (2, 6 and 11).

533

534 **Table 3.** Thickness, moisture content (MC), water solubility (WS), water vapor

535 permeability (WVP) and glass transition temperature (Tg) of gelatin-based films (G)

536 added or not with methyl orange (MO), neutral red (NR), and bromocresol green (BCG)

537 at pH 2, 6 and 11.

538

539 **Supplementary Table.** CIE-Lab color parameters (L*, a* and b*) of gelatin (G) films

540 added with methyl orange (MO), neutral red (NR) and bromocresol green (BCG) at pH

541 2, 6, and 11 and their corresponding responses against acid or alkali liquid, gaseous and

542 semisolid media.

543

Table 1. Chemical structure, pKa, pH dependence color, and λ_{max} in the visible region of methyl orange (MO), neutral red (NR) and bromocresol green (BCG), used in this manuscript as pH indicators [*].

Acid-base indicator	Chemical structure	λ_{max}	pKa	Color change
Methyl Orange (MO)		507-522 nm 464 nm	3.7	Red at pH<3.0 Yellow at pH>4.4
Neutral Red (NR)		529-544 nm 454 nm	7.4	Red at pH<6.8 Yellow at pH>8.0
Bromocresol Green (BCG)		423-444 nm 617 nm	4.6	Yellow at pH<3.8 Blue at pH>5.4

[*] Data from Sabnis [29].

Table 2. CIE-Lab color parameters (L^*, a^* and b^*) and total color difference (ΔE^*) of gelatin-based films added or not with different acid-base indicators (MO, NR, BCG) obtained at different pH (2, 6 and 11).

Film	pH	L^*	a^*	b^*	ΔE^*
G	**2**	$94.41 \pm 0.21^{a/x}$	$-0.79 \pm 0.06^{a/x}$	$2.10 \pm 0.17^{a/x}$	$2.06 \pm 0.12^{a/x}$
	6	$93.35 \pm 0.55^{a/x}$	$-0.94 \pm 0.07^{a/x}$	$2.70 \pm 0.61^{a/x}$	$1.85 \pm 0.52^{a/x}$
	11	$93.87 \pm 0.58^{a/x}$	$-1.07 \pm 0.07^{a/x}$	$2.05 \pm 0.11^{a/x}$	$2.64 \pm 0.22^{b/x}$
G+MO	**2**	$80.30 \pm 0.50^{a/y}$	$26.50 \pm 0.04^{a/y}$	$61.70 \pm 1.62^{a/y}$	$11.8 \pm 0.09^{a/y}$
	6	$79.67 \pm 0.28^{a/y}$	$17.11 \pm 0.26^{b/y}$	$65.27 \pm 0.08^{b/y}$	$11.30 \pm 0.05^{b/y}$
	11	$47.02 \pm 0.29^{b/y}$	$58.34 \pm 0.37^{c/y}$	$-4.17 \pm 0.18^{c/y}$	$2.41 \pm 0.29^{c/x}$
G+NR	**2**	$50.63 \pm 0.72^{a/z}$	$58.01 \pm 0.52^{a/z}$	$4.64 \pm 0.37^{a/x}$	$5.48 \pm 0.17^{a/z}$
	6	$62.69 \pm 0.64^{b/z}$	$23.12 \pm 0.92^{b/z}$	$25.85 \pm 0.49^{b/z}$	$5.18 \pm 0.17^{b/z}$
	11	$64.93 \pm 0.98^{c/z}$	$16.81 \pm 0.85^{c/z}$	$20.32 \pm 0.74^{c/z}$	$3.25 \pm 0.10^{c/y}$
G+BCG	**2**	$91.53 \pm 0.46^{a/w}$	$-5.73 \pm 0.02^{a/w}$	$31.57 \pm 0.84^{a/z}$	$6.18 \pm 0.13^{a/w}$
	6	$57.41 \pm 0.23^{b/w}$	$-10.66 \pm 1.13^{b/w}$	$-32.33 \pm 1.89^{b/w}$	$12.94 \pm 0.50^{b/z}$
	11	$43.33 \pm 1.24^{c/w}$	$-5.21 \pm 0.42^{c/w}$	$-47.01 \pm 0.48^{c/w}$	$14.63 \pm 0.09^{c/z}$

Reported values for each gelatin film are means ± standard deviation (n=9). Different letters (a, b, c, d) in the same column indicate significant differences (p<0.05) among the different acid-base indicators for the same pH of film-forming dispersion, according to Tukey´s test. Different letters (w, x, y, z) in the same column indicate significant differences (p<0.05) among the different pH of film-forming dispersion for the same film formulation, according to Tukey´s test.

Table 3. Thickness, moisture content (MC), water solubility (WS), water vapor permeability (WVP) and glass transition temperature (Tg) of gelatin-based films (G) added or not with methyl orange (MO), neutral red (NR), and bromocresol green (BCG) at pH 2, 6 and 11.

Film	pH	Thickness (µm)	MC (%)	WS (%)	WVP $*10^{11}$ ($gH_2O/s.m.Pa$)	Tg (^oC)
G	2	$49.5 \pm 3.9^{a/x}$	$19.2 \pm 0.5^{a/x}$	$49.6 \pm 1.6^{a/x}$	$7.63 \pm 0.84^{a/x}$	$-7.9 \pm 0.7^{a/x}$
	6	$51.0 \pm 3.0^{a/x}$	$22.1 \pm 0.6^{a/y}$	$37.6 \pm 2.7^{a/y}$	$6.54 \pm 0.34^{a/x}$	$-6.3 \pm 2.0^{a/x}$
	11	$47.8 \pm 3.4^{a/x}$	$21.5 \pm 0.3^{a/y}$	$37.6 \pm 1.8^{a/y}$	$7.96 \pm 0.36^{ab/x}$	$-6.8 \pm 0.7^{a/x}$
G+MO	2	$45.4 \pm 2.2^{a/x}$	$16.9 \pm 0.8^{b/x}$	$30.7 \pm 2.9^{b/x}$	$8.28 \pm 0.86^{a/x}$	$-7.3 \pm 1.0^{a/x}$
	6	$48.1 \pm 2.3^{a/x}$	$16.3 \pm 0.5^{b/x}$	$23.2 \pm 1.4^{b/y}$	$7.00 \pm 0.96^{a/x}$	$-5.1 \pm 0.5^{b/x}$
	11	$51.1 \pm 3.0^{a/x}$	$17.3 \pm 0.3^{b/x}$	$15.2 \pm 0.1^{b/z}$	$6.71 \pm 0.19^{a/x}$	$-6.9 \pm 0.5^{a/x}$
G+NR	2	$49.7 \pm 3.3^{a/x}$	$17.4 \pm 0.6^{b/x}$	$53.5 \pm 4.4^{a/x}$	$8.90 \pm 0.94^{a/x}$	$-7.7 \pm 0.5^{a/x}$
	6	$50.2 \pm 1.8^{a/x}$	$17.5 \pm 1.1^{b/x}$	$38.1 \pm 1.9^{a/y}$	$8.83 \pm 0.75^{a/x}$	$-5.7 \pm 1.2^{a/x}$
	11	$50.7 \pm 1.9^{a/x}$	$16.5 \pm 0.1^{b/x}$	$34.1 \pm 1.0^{a/y}$	$8.58 \pm 0.78^{bc/x}$	$-6.7 \pm 0.1^{a/x}$
G+BCG	2	$46.0 \pm 2.1^{a/x}$	$20.5 \pm 0.7^{a/x}$	$51.3 \pm 0.9^{a/x}$	$9.12 \pm 0.13^{a/xy}$	$-6.2 \pm 1.1^{a/x}$
	6	$49.5 \pm 3.7^{a/x}$	$23.3 \pm 1.2^{a/y}$	$21.5 \pm 0.5^{b/y}$	$8.62 \pm 0.25^{a/x}$	$-4.2 \pm 0.5^{b/x}$
	11	$49.4 \pm 6.5^{a/x}$	$20.3 \pm 0.2^{a/x}$	$49.8 \pm 5.6^{c/x}$	$9.90 \pm 0.70^{c/y}$	$-6.5 \pm 1.1^{a/x}$

Reported values for each gelatin film are means ± standard deviation ($n=9$ for thickness; $n=3$ for MC, WS and WVP; $n=2$ for Tg). Different letters (a, b, c) in the same column indicate significant differences ($p<0.05$) among the different acid-base indicators for the same pH of film-forming dispersion, according to Tukey´s test. Different letters (x, y, z) in the same column indicate significant differences ($p<0.05$) among the different pH of film-forming dispersion for the same film formulation, according to Tukey´s test.
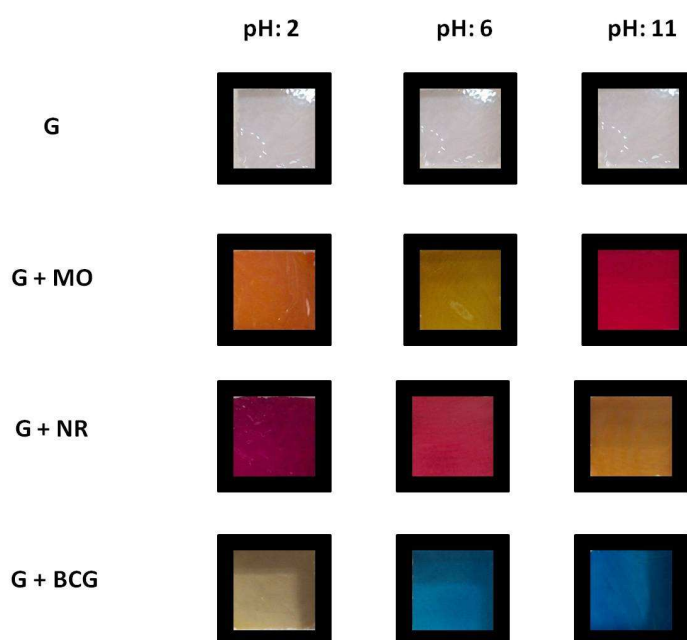
Figure 1. Appearance of control gelatin-based films (G) and those added with methyl orange (G+MO), neutral red (G+NR), and bromocresol green (G+BCG) at pH 2, 6 and 11.
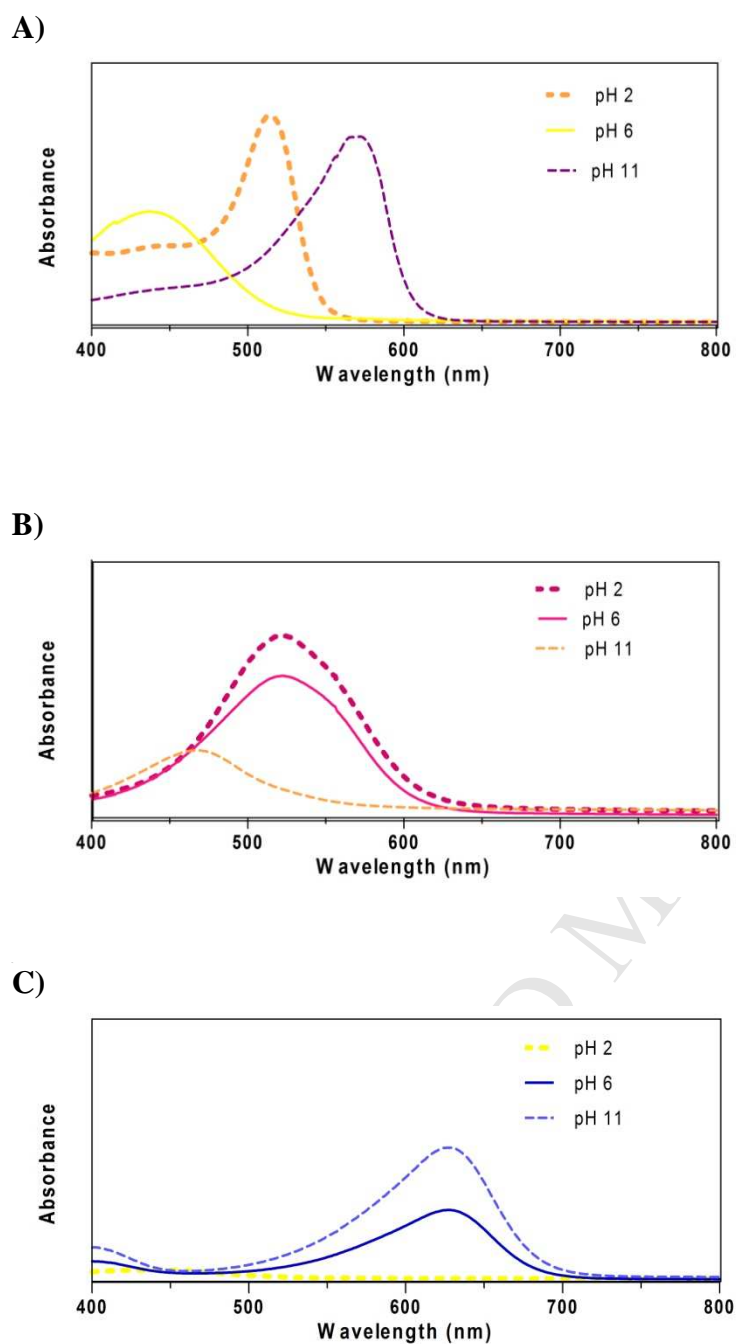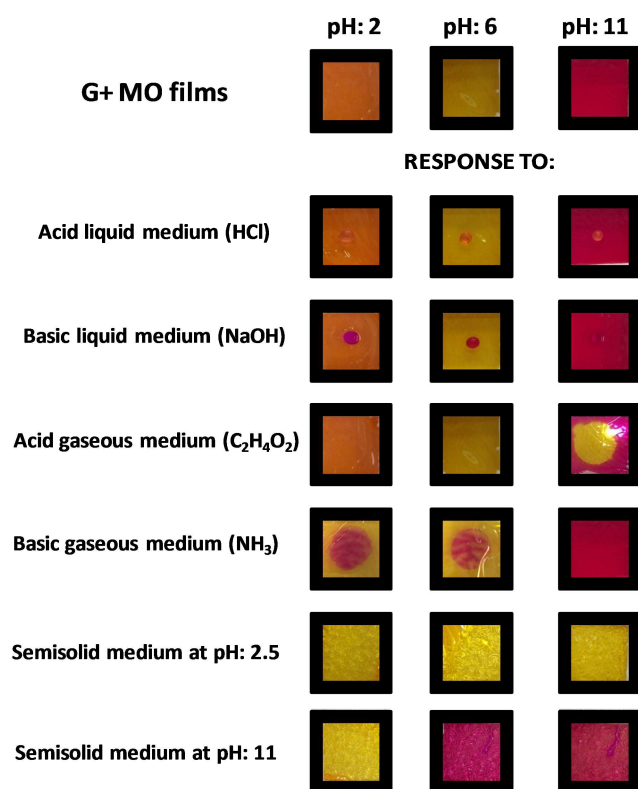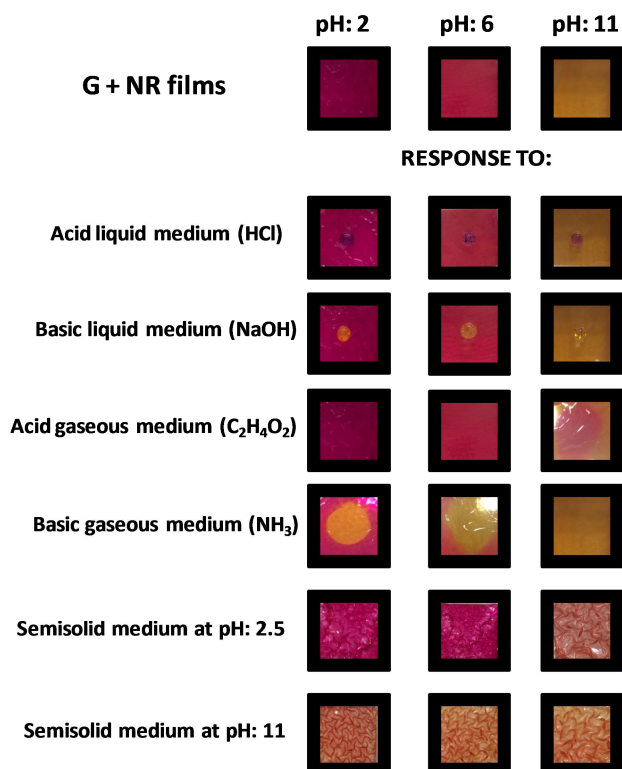
A)

B)

C)

Figure 2. Visible absorption spectra (400-800 nm) of gelatin-based films added with methyl orange (**A**), neutral red (**B**) and bromocresol green (**C**) at pH 2, 6, and 11 respectively.
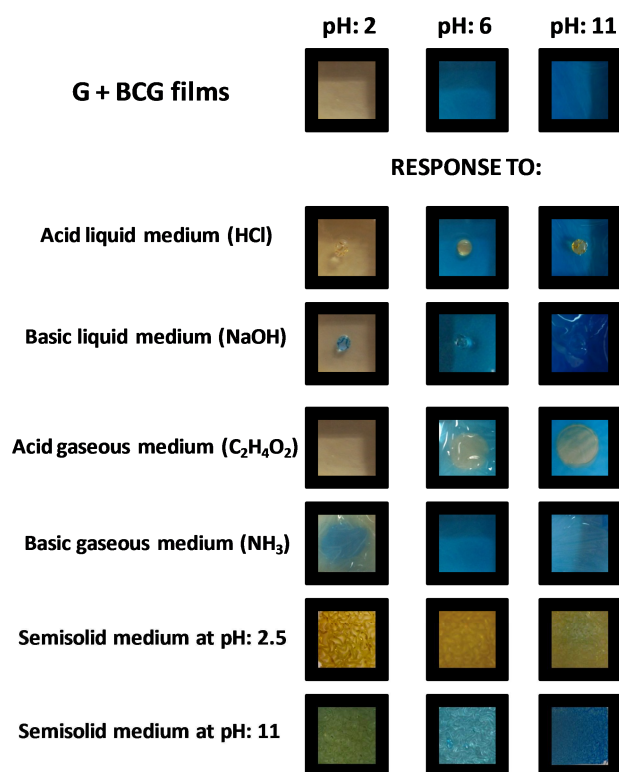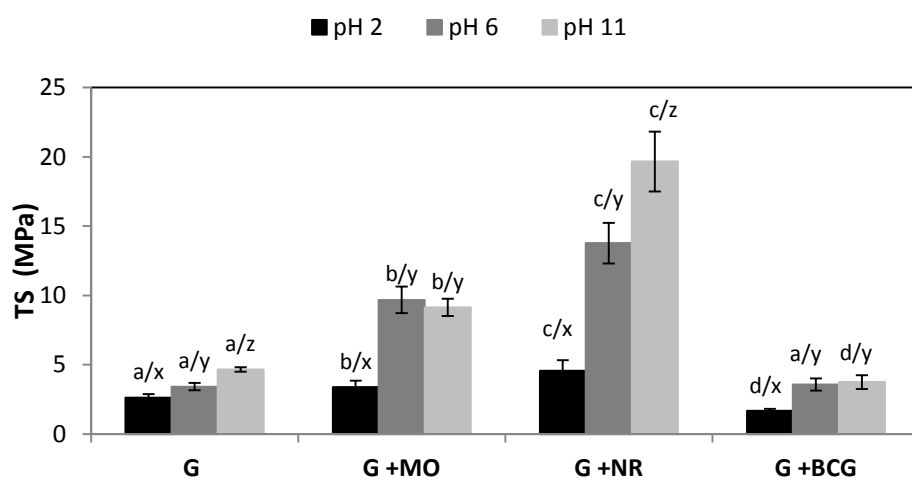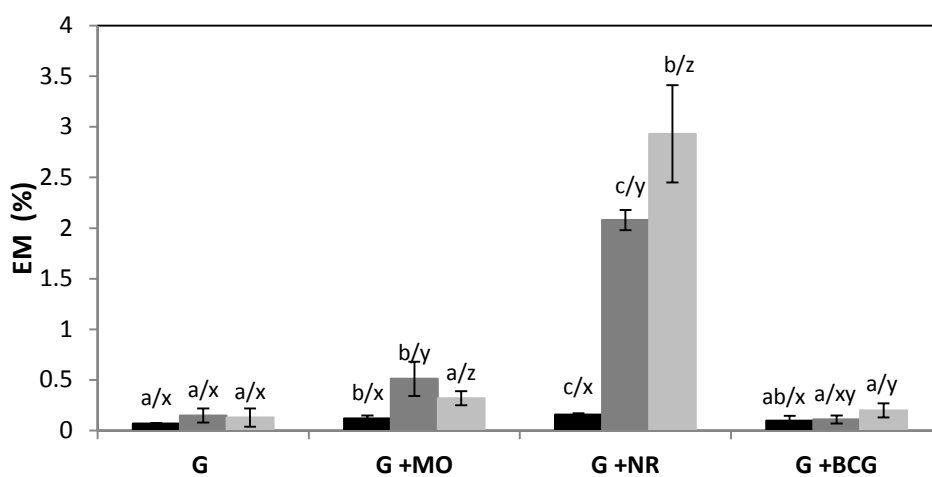
A)

B)

C)

Figure 3. Response of gelatin-based films added with methyl orange (G+MO, **A**), neutral red (G+NR, **B**), and bromocresol green (G+BCG, **C**) at pH 2, 6 and 11 after being in contact with liquid, gaseous and semisolid media of different pHs.

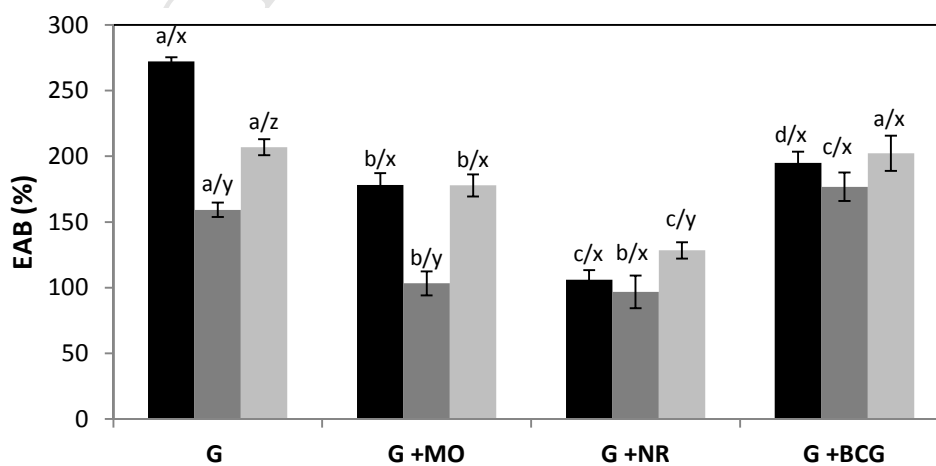**A)**

B)

C)

Figure 4. Mechanical properties of gelatin-based films obtained at different pH (2, 6 and 11) added or not with different acid-base indicators (MO, NR, and BCG). **A**) Tensile strength (TS). **B**) Young´s modulus (EM). **C**) Elongation at break (EAB).

Reported values for each gelatin film are means ± standard deviation (n=12). Different letters (a, b, c, d) indicate significant differences (p<0.05) among the different acid-base indicators for the same pH of film-forming dispersion, according to Tukey´s test. Different letters (x, y, z) indicate significant differences (p<0.05) among the different pH of film-forming dispersion for the same film formulation, according to Tukey´s test.

Highlights

- Smart gelatin films added with synthetic acid-base indicators were developed
- Films modified their color after being in contact with media at different pHs
- Films´ response was evaluated against gaseous, liquid and semisolid media
- Protein matrix didn't interfere with the discoloration of the acid-base indicators
- Acid-base indicator´s presence affected the physicochemical properties of films